COMPUTATIONAL AND SENSITIVITY ANALYSIS OF A DUAL PURPOSE SOLAR CHIMNEY FOR BUILDINGS

Layeni A. T.[1], Waheed M. A.[2], Adewumi B. A.[3], Nwaokocha C. N.[1,4]*, Sharifpur M.[4], Tongo O. O.[5], Okeze R. C.[6], Mboreha C. A.[7]

[1]*Department of Mechanical Engineering, Olabisi Onabanjo University, Ago-Iwoye, Nigeria.*
[2]*Department of Mechanical Engineering, Federal University of Agriculture, Abeokuta, Nigeria.*
[3]*Department of Agricultural Engineering, Federal University of Agriculture, Abeokuta, Nigeria.*
[4]*Department of Mechanical & Aeronautical Engineering, University of Pretoria, Pretoria, South Africa.*
[5]*Department of Architecture, Olabisi Onabanjo University, Ago-Iwoye, Nigeria.*
[6]*Department of Mechatronics Engineering, Federal Polytechnic, Ilaro, Nigeria.*
[7] *Department of Aeronautical Engineering, Nanjing University of Aeronautics and Astronautics, Jiangsu, Nanjing, China*

*__Corresponding Author:__ collinsnwaokocha@gmail.com

Abstract

The solution(s) to issues of electric power availability is a great concern in many places in both underdeveloped and developing countries. A solution to this problem is proposed in the use of the Solar Chimney (SC). In this study the potentials of using the Solar Chimney is analysed as a means of improving the power problem and providing ventilation at the same time in building in Nigeria. The Solar chimney (SC) being a natural flow device that uses solar irradiation to cause buoyancy in flowing air by means of the addition of heat, thereby converting the solar thermal energy of the sun into kinetic energy in the flowing air. The SC had been developed for the purpose of ventilation for over two millennia now, while the SC has also been developed in recent time for power generation. In this study computational analysis was carried out using the ANSYS Fluent CFD package together with a statistical package "Design Expert" to carryout sensitivity analysis to determining the potentials of the SC system for buildings. A 2^3 factorial experiment was simulated and analysed on a 4m x 4m x 4m room. Results revealed by the simulated factorial experiments that the effect of interactions of parametric factors of the SC, chimney height, width and Solar heat flux, were of great importance. The power output from the SC is about 25 W/m^2, with a channel velocity of 1.5 m/s. The room temperature was maintained as its initial value of 300 K, with an increase in room average velocity to about 1.5 m/s..

***Keywords**:* Solar Chimney (SC); Solar Chimney Power Plant (SCPP); CFD; Passive Ventilation; Trombe wall; Wind Turbine.

Highlights

- The rising global need for clean energy resource;
- Analysis of the potentials of Solar Chimney as a means of improving the power problem and providing ventilation at the same time in building;
- Computational analysis using the ANSYS Fluent CFD package;
- Sensitivity analysis using Design Expert;
- Development and optimisation of a Solar Chimney (SC) model for the dual purpose of passive ventilation and renewable power generation in buildings in tropical conditions was achieved.

NOMENCLATURE

A area (m^2)
A_c cross section area of chimney (m^2)
Cp specific heat at constant pressure (J/kg K)
Δp total pressure difference between the chimney base and the ambient or pressure loss of a component (Pa)
D diameter (m)
e height of the cover (m)
f wall friction factor
G global solar radiation (W/m^2)
g gravitational acceleration (m/s^2)
H chimney height (m)
h heat transfer coefficient (W/m^2 K)
I solar radiation (W/m^2)
k thermal conductivity (W/m K)
m flow rate (kg/s)
Nu Nusselt number
Pr Prandtl number
P power (W/m^2)
p pressure (Pa, N/m^2)
Q heat output (J/s)
Ra Rayleigh number
R_{coll} collector radius (m)
Re Reynolds number
T temperature (K)
t time (s)
U total heat transfer coefficient from chimney airflow to atmospheric air (W/m^2-K)
U_∞ convective heat transfer coefficient between the chimney wall and the airflow inside the solar chimney (W/m^2-K)
U_f convective heat transfer coefficient between the chimney wall and atmospheric air (W/m^2-K)
V Air velocity (m/s)

Greek symbols
α absorptivity
β coefficient of thermal expansivity
β slope (degree)
τ transmitivity
δ thickness (m)
ε emissivity
η energy conversion efficiency (%)
γ lapse rate of temperature (K/m)
ρ density (kg/m^3)
μ viscosity of air (kg/m s)

1 INTRODUCTION

In the world today, fossil fuels are the main sources of energy. The present energy production and use of fossil fuels have added to the increasing carbon footprint globally, which has contributed to global warming and other environmental issues. These issues have necessitated research into other sources of energy that are renewable. It is noted that insufficient energy supplies may lead to high energy costs, which invariably leads to a low standard of living as well as to poverty. There is therefore a need for a switch to renewable sources of energy. According to current research, the use of wind turbines for power generation is increasing globally. The wind power generation systems have installed capacity of 238,000 Megawatts (MW) worldwide as of 2011 (Renewables 2011 Global Status Report, 2011; Morales, 2012), while a global capacity of 60.4 Gigawatts (GW) as of 2019 was reported in the Global Wind Report 2019 (Lee and Zhao, 2020). Moreover, several renewable energy schemes are extensive and in urban areas. However, renewable energy technologies are also applicable in remote and rural areas. Climate change issues, increasing oil prices, and increasing government involvement around the world are some of the driving forces for the increased commercialization of renewable energy in many developed and developing countries. According to a 2011 projection, renewable (solar energy) power plants may generate almost all the needed electricity capacity worldwide within the next 50 years, radically reducing the greenhouse gas emissions harmful to the environment (Ben Sills, 2011).

Schlaich and Schiel (2000) stated that "Sensible technology for the use of solar power must be simple and reliable, accessible to the technologically less developed countries that are sunny and often have limited raw materials resources, should not need cooling water or produce waste heat and should be based on environmentally sound production from renewable materials." This is where other technology of harnessing solar energy is sought after, that will produce the required energy at a cost lower than that of the present cost of Photo Voltaic (PV) solar energy technology. The solar chimney technology is observed to meet the above conditions, which will be a step towards achieving a worldwide solar energy economy (Layeni *et al*,2020a). Schlaich and Schiel (2000) stated that feasibility reports showed that rated capacities of 100 and 200 MW of solar chimneys generate energy at comparable costs to conventional power generation plants. This is a major motivation for the development of the solar chimney energy system.

The SC has also been applied in providing ventilation for buildings. Passive ventilation of buildings through the use of the SC has been accomplished with solar-driven stack effect and buoyancy-induced airflow. Gontikaki *et al*.(2010) noted that the harnessing of renewable and sustainable energy sources with respect to the buildings' functional demand for cooling, heating, ventilation, etc., contributes to energy savings, and improving the present problems associated with conventional energy practices. Passive ventilation of buildings assists greatly to save the energy otherwise spent for mechanical ventilation, which can be achieved successfully with the use of a SC ventilation system.

The present state of technology of using the SC as a combined ventilation and power system has been explored and published by researchers (Layeni *et al* 2015, Layeni *et al* 2020a and Layeni *et al* 2020b)); however, this research attempts to use a different methodology to study the combined effects of the major parameters affecting the performance of the SC.

1.1 Solar Chimney Ventilation System

Literature abounds on the use of chimneys/solar collectors for various use such as agricultural produce drying and buildings' heating and ventilating system amongst other passive systems (Bilgen and Michel, 1979; Bar-Cohen and Krauss, 1988; Ekechukwa and Norton, 1999; Schlaich

and Schiel, 2000; Nouanégué and Bilgen, 2009). Gontikaki *et al.* (2010) noted that a SC ventilation system differs from a conventional chimney with least a wall made of transparent material (glass), which allows solar thermal energy to heat up the walls of the chimney (Figure 1). This increases the air temperature inside the SC as heat is transferred from the walls to the air, and the air rises due to the buoyancy effect. This effect results in the SC pulling air from inside the building, going out through the SC, and replaced by fresh air through fenestrations within the building, thus achieving natural ventilation. Induced ventilation flow rates and air temperatures within and outside the channel are thus performance indicators of the SC.
Burek and Habeb (2007) reported in their experimental study of thermos-siphoning air heaters that the mass flow rate was a function of both the heat flux and chimney depth; and that the thermal efficiency of the system was only a function of heat flux.

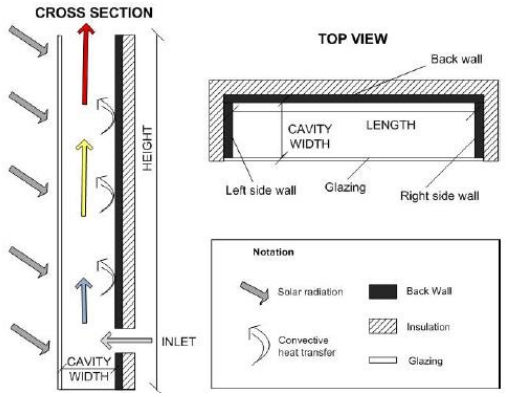

Figure 1. Orthographic Views of a Solar Chimney (Gontikaki et al. 2010)

Gontikaki et al. (2010) carried out sensitivity analysis on major design parameters of the SC to determine the system's performance. They stated that the most dominant parameters can be categorised as geometrical parameters, which include the chimney's height, gap and width; construction parameters, including the type of glass, insulation, etc.; and climatic parameters, which include solar radiation, wind, etc. it was also noted that wind was found to be the second most significant climatic parameter, as it creates negative or positive pressures at the outlet of the SC and thus obstruct or enhance the airflow. The experimental study of Arce *et al*. (2009) showed that the highest airflow rates corresponded with the maximum recorded wind velocity.
Alwetaishi (2017) examined the effect of glazing to wall ratio in different microclimate regions in Saudi Arabia. Investigation on the impact of changing glazing to wall ratio in different climatic zones was done. The results showed that the south-facing classrooms receive the most solar radiation. Further results noted that a larger area of glazing in a hot and humid climate is more favourable to have the same effect as in a hot and dry climate. It is recommended that a 10% glazing to wall ratio be applied in both hot and dry, and hot and humid climates to walls facing the south and east directions as they receive the most amount of heat in all locations. And consequently, the glazing in these directions should be minimised.

1.2 Solar Chimney Power Plant

Schlaich and Schiel (2000) indicated that the Solar Chimney Power Plant's most important elements are the chimney, solar collector, and turbine (Figure 2). The SC power plant combines these elements to generate power (Schlaich and Schiel, (2000); Liu et al., (2005); Zhou et al., (2009); Pretorius and Kröger, (2006)). In the solar collector, an absorber on the ground is heated

up by solar radiation, which in turn heats up the air in the collector. The hot energised air rises up through the chimney section due to the density and temperature difference of air at the base of the chimney and the environment. As the hot energised air rises, it drives turbines mounted at the base of the chimney, which is connected to an electric power generator.

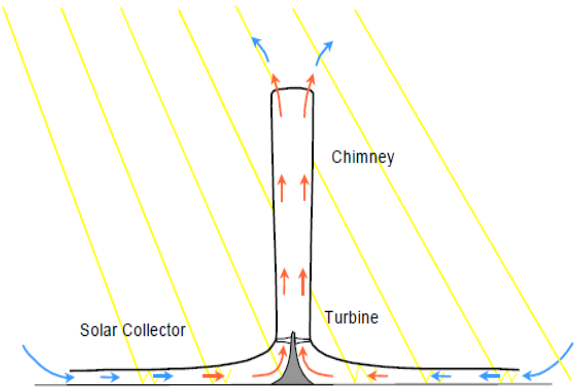

Figure 2. The solar chimney power plant (Schlaich and Schiel, 2000)

Zhou *et al*. (2009) found that the results established by the pilot, Manzanares prototype, showed that the maximum power output of 102.2 kW was obtained for the optimal chimney height of 615 m, which is a lower height to the maximum chimney height that produced a power output of 92.3 kW. Pretorius and Kröger, (2009) reported that windy conditions may impair the performance of the SC plant considerably, while nocturnal inversions in temperature cause significant reductions in night-time output.

1.3 PRESENT STUDY

The review of the SC technologies showed that there are some similarities in the performance analysis of both systems: an increase in chimney height improves the performance of both systems, however, according to Schlaich (1995) no physical optimum SC power plant exists since an increase in height always produces an increase in power output, while the chimney height of the SC ventilation system can be optimised with other parametric parameters (Pretorius, 2007; Pretorius and Kröger, 2007). This and other contrary effects, like reverse flow at some geometries, which may affect the performance of the combined ventilation and power system need to be investigated to ascertain the workability of the combined system. The present study attempts to investigate these relationships by carrying out a factorial simulated experiment on the combined effects of major parameters on the performance of the SC, thus setting the pace for the developments of the combined SC technology using this methodology.

Physical Model

The atmospheric conditions used in this analysis is based on the Abeokuta area, with the ambient average temperature of 27^{O} C, the mean air velocity of 1.2 m/s, the atmospheric pressure of 1013mb (Ikhile, (2012)), and the mean solar radiation of about 200 W/m^2 (Nwofe, (2014)). The set-up of the model is as presented in Figure. 3, with the SC consisting of a horizontal solar collector and a chimney section with glass used as wall material and serves as a vertical solar

collector. Solar energy enters through the glass wall and heats up the air inside the horizontal and vertical (solar chimney) solar collectors.

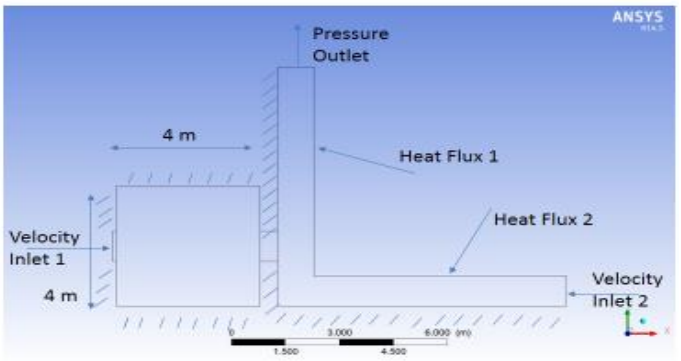

Figure 3. Physical Model of the Combined Ventilation and Power SC

2 RESEARCH METHODOLOGY

The design and methodology selected has been adopted based on the standard internationally applied scientific procedure and tested mathematical model and CFD solutions in the field of both Ventilation and Power Solar chimney. This is presented as follows:

2.1 Experimentation

The Design of Experiment (DOE) methodology using the 2^K Factorial experimental design (Tables 1 and 2) was applied for the study. The DOE setup experiments were then simulated using the ANSYS Fluent CFD package.

Table 1. Design Factors for the Experimental Setup

Level	Height of Solar Chimney (HSC) (m)	Breadth of Solar Chimney (BSC) (m)	Solar Heat Flux (W/m^2)	Wind Speed (m/s)
Low (-)	4	1	200	0.05
High (+)	8	2	1,000	0.05

Table 2. Factorial Experiment Adopted (Two (2) Levels, Three (3) Factors)

Experiment Run	HSC (m)	BSC (m)	Solar Heat Flux (W/m^2)
1	4	1	200
2	8	1	200
3	4	2	200
4	8	2	200
5	4	1	1,000
6	8	1	1,000
7	4	2	1,000

8	8	2	1,000

In all the literature reviewed, no one used the scientific method of design of experiment (factorial experiment) to set up their experiments or other statistical method that can reveal any interaction(s) among the independent factors affecting the performance of either the SCPP or SCVS, which may be a reason why optimisation models developed are dependent on the cost as a variable.

2.2 Computational Fluid Dynamics (CFD) Analysis

The ANSYS FLUENT software was used for CFD simulation and analysis of the study. The mathematical models are the 3-D Navier-Stokes equation, the continuity and momentum equations coupled with the energy equation, and the equation of state for the heat transfer analysis of the system. Additional transport equations were modelled for turbulent flow (ANSYS FLUENT Theory Guide, 2011).

$$\frac{\partial \rho}{\partial t} + \frac{\partial}{\partial x_i}(\rho u_i) = 0 \quad (1)$$

$$\frac{\partial}{\partial t}(\rho u_i) + \frac{\partial}{\partial x_j}(\rho u_i u_j) = -\frac{\partial P}{\partial x_i} + \frac{\partial}{\partial x_j}\left[\mu\left(\frac{\partial u_i}{\partial x_j} + \frac{\partial u_j}{\partial x_i} - \frac{2}{3}\delta_{ij}\frac{\partial u_l}{\partial x_l}\right)\right] \quad (2)$$

Equations (1) and (2) are the Reynolds-Averaged Navier-Stokes (RANS) equations. Equations (1) and (2) have the same form as the instantaneous Navier-Stokes equations, with velocities and other solution variables represented by ensemble (time)-averaged values. Reynolds stresses ($-\rho\overline{u_i' u_j'}$) are modelled in order to close Equation 2.

The Boussinesq hypothesis is used in relating the Reynolds stresses to the mean velocity gradients as required by the Reynolds-averaged method for turbulence modelling. This requires that the Reynolds stresses, as presented in Equation (2), are appropriately modelled:

$$-\rho\overline{u_i' u_j'} = \mu_t\left(\frac{\partial u_i}{\partial x_j} + \frac{\partial u_j}{\partial x_i}\right) - \frac{2}{3}\left(\rho k + \mu_t\frac{\partial u_k}{\partial x_k}\right)\delta_{ij} \quad (3)$$

The k – Ɛ turbulence model uses the Boussinesq hypothesis, which is applied in this study (Peri *et al*., 2011). All the simulations of the airflow use the k– Ɛ turbulence model. The typical k – Ɛ turbulence model is based on the model transport equations for the turbulent kinetic energy (k) and the turbulent kinetic energy dissipation rate (Ɛ).

$$\frac{\partial}{\partial t}(\rho k) + \frac{\partial}{\partial x_i}(\rho k u_i) = \frac{\partial}{\partial x_j}\left(\left(\mu + \frac{\mu_t}{\sigma_k}\right)\frac{\partial k}{\partial x_j}\right) + G_k + G_b - \rho\varepsilon + S_k \quad (4)$$

$$\frac{\partial}{\partial t}(\rho \varepsilon) + \frac{\partial}{\partial x_i}(\rho \varepsilon u_i) = \frac{\partial}{\partial x_j}\left(\left(\mu + \frac{\mu_t}{\sigma_\varepsilon}\right)\frac{\partial \varepsilon}{\partial x_j}\right) + C_{l\varepsilon}(G_k + C_{3\varepsilon}G_b) - C_{2\varepsilon}\rho\frac{\varepsilon^2}{k} + S_\varepsilon \quad (5)$$

From Equations (4) and (5) above, G_k denotes the generation of turbulent kinetic energy due to the mean velocity gradients, and G_b denotes the generation of turbulent kinetic energy due to buoyancy.

Natural Convection and Buoyancy-Driven Flows Theory

Buoyancy-driven flows are known as natural convection (or mixed-convection) flows and are modelled by ANSYS FLUENT. The significance of buoyancy forces in a mixed convection flow can be determined by the ratio of the Grashof and Reynolds numbers given by:

$$\frac{Gr}{Re^2} = \frac{g\beta\Delta TL}{v^2} \quad \textbf{(6)}$$

A strong buoyancy aided flow is expected when this ratio tends towards or exceeds one. Conversely, if the ratio is very small, buoyancy forces may be disregarded in the simulation. In pure natural convection, the intensity of the buoyancy-induced flow is determined by the Rayleigh number:

$$Ra = \frac{g\beta\Delta TL^3\rho}{\mu\alpha} \quad \textbf{(7)}$$

where β is the thermal expansivity given by,

$$\beta = -\frac{1}{\rho}\left(\frac{\partial\rho}{\partial T}\right)_p \quad \textbf{(8)}$$

and α is the thermal diffusivity given by,

$$\alpha = \frac{k}{\rho c_p} \quad \textbf{(9)}$$

2.3 Scope

The scope of the research simulation is limited to a 4 m x 4 m x 4 m room, Chimney dimension of between 1 m x 1 m x 4 m (minimum) – 1 m x 2 m x 8 m (maximum), (Horizontal) Solar Collector dimension between 8 m x 1 m x 1 m (minimum) – 8 m x 2 m x 1 m (maximum), Solar irradiation (solar heat flux) between 200 W/m^2 (minimum) – 1,000 W/m^2 (maximum), Ambient temperature of 27^O C (300K) and Wind condition of 0.05 m/s; Wind effect of 1.0 m/s was also applied.

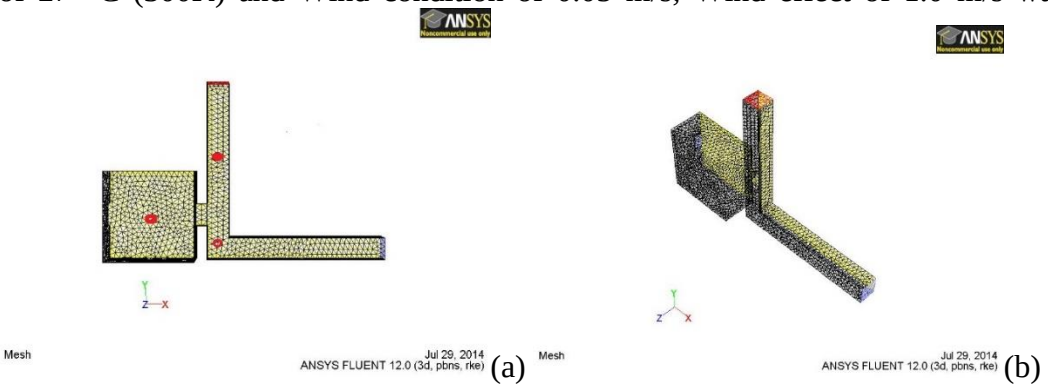

Figure 4. (a) Side View showing the mesh and Analysis Points (b) Pictorial View of the Experimental Model Mesh

3 RESULTS AND ANALYSIS

3.1 Verification and Validation of Results

The simulated model was verified taking values of the Nu for different grid refinements from 1,332 Nodes and 2583 Elements with Nu of 164.3 to 14,975 Nodes and 41,516 Elements with Nu of

154.2 (Table 3). It was observed that the difference in Nu of a grid size with a previous lower grid size became less than one (0.62) at a grid size of 14,969 nodes and 41,472 elements, and on the next refinement a difference of 0.2 was observed.

The model was validated with experimental results (Figure 6) of the effect of heat flux on the air flow rate from Chen *et al*. (2003) and simulated results (Figure 5) of mass flow rate from Miyazaki *et al*. (2006). The present study has a deviation of 2.5% with the experimental results of Chen *et al*. (2003) while the deviation from the simulated results of Miyazaki *et al*. (2006) was found to be about 7.4%. The higher value from the simulated results would have been as a results of the inherent cumulative errors of the two simulations. However, the model showed a close agreement with experimental results.

Table 3. Grid Refinement

GRID	Relevance Centre	Smoothing	Nodes	Elements	Nusselt Number Nu	% Difference	% Deviation from Max
1	Coarse	Medium	1332	2583	164.3147		6.53522
2	Coarse	High	1333	2587	163.0449	0.77	5.71193
5	Medium	High	4,812	11,373	162.101	0.58	5.09994
4	Medium	Medium	4,820	11,356	162.4545	-0.22	5.32914
3	Medium	Low	4,854	11,405	162.5303	-0.05	5.37828
6	Fine	Low	14,648	40,487	155.7365	4.18	0.97345
7	Fine	Medium	14,969	41,472	154.7678	0.62	0.34538
8	Fine	High	14,975	41,516	154.2351	0.34	0

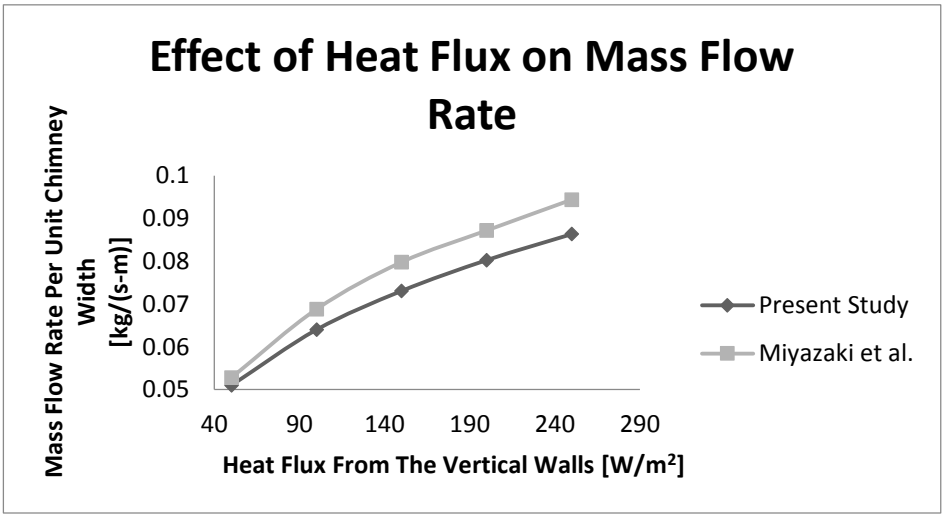

Figure 5. The Effect of Heat Flux on Mass Flow Rate of the Present Study in Comparison with CFD Results from Miyazaki *et al.* (2006)

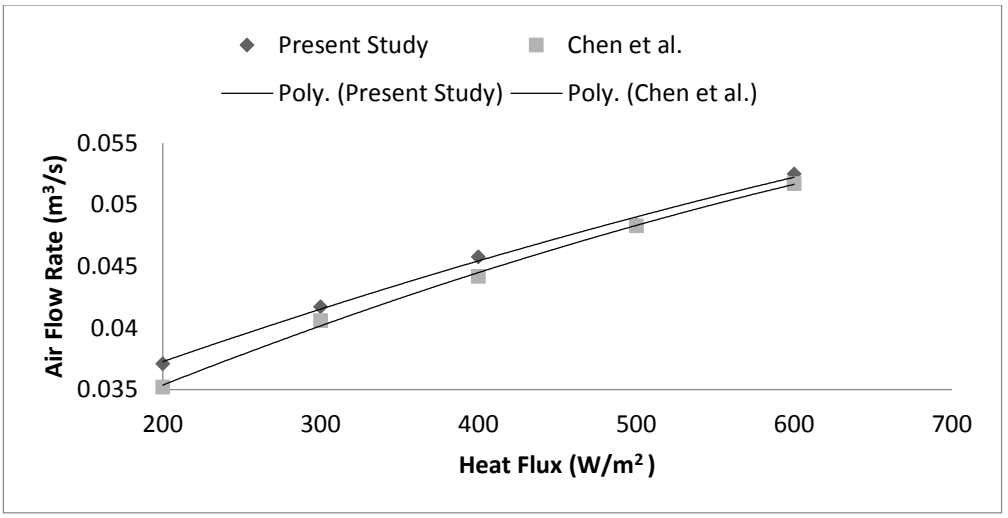

Figure 6. Comparison of the present simulated airflow rate through the chimney with 200 mm gap with experimental results from Chen et al. (2003) at different input solar heat flux.

3.2 Analysis of Results

For the present study the analysis procedure for the DOE 2^K Factorial was adopted and the Statistical Package, "Design Expert" was used for the analysis.

Equations of the Response Factors Developed

$$V_1 = 0.082 - 9.12 \times 10^{-3}H - 8.25 \times 10^{-5}S + 1.25 \times 10^{-5}HS \quad (10)$$

$$V_2 = 0.195 - 0.063B - 4.69 \times 10^{-5}S + 2.5 \times 10^{-5}BS \quad (11)$$

$$V_3 = 0.105 - 3.97 \times 10^{-3}H - 1.07 \times 10^{-4}S + 1.42 \times 10^{-5}HS \quad (12)$$

$$T_1 = 273 + 4H + 24.5B - 3.38HB \quad (13)$$

$$T_2 = 288.6 + 1.5H + 2.5B + 0.023S - 0.25HB - 6.2 \times 10^{4}HS + 0.025BS \quad (14)$$

$$T_3 = 295.3 + 0.057S \quad (15)$$

Chimney Height – H, (Horizontal) Solar Collector Breadth – B, Solar Heat Flux - S

V_1 = Room Average Velocity, V_2 = Chimney Average Velocity, V_3 = Horizontal Solar Collector Average Velocity, T_1 = Room Average Temperature, T_2 = Chimney Average Temperature, T_3 = Horizontal Solar Collector Average Temperature

Figures 7 and 8 show the contour plots for velocity and temperature, and also the velocity vector for the minimum and maximum chimney heights. The velocity profile for the minimum chimney height shows increased velocity in the chimney in comparison to the room velocity. While the maximum height chimney shows an improved room velocity consequently a better temperature.

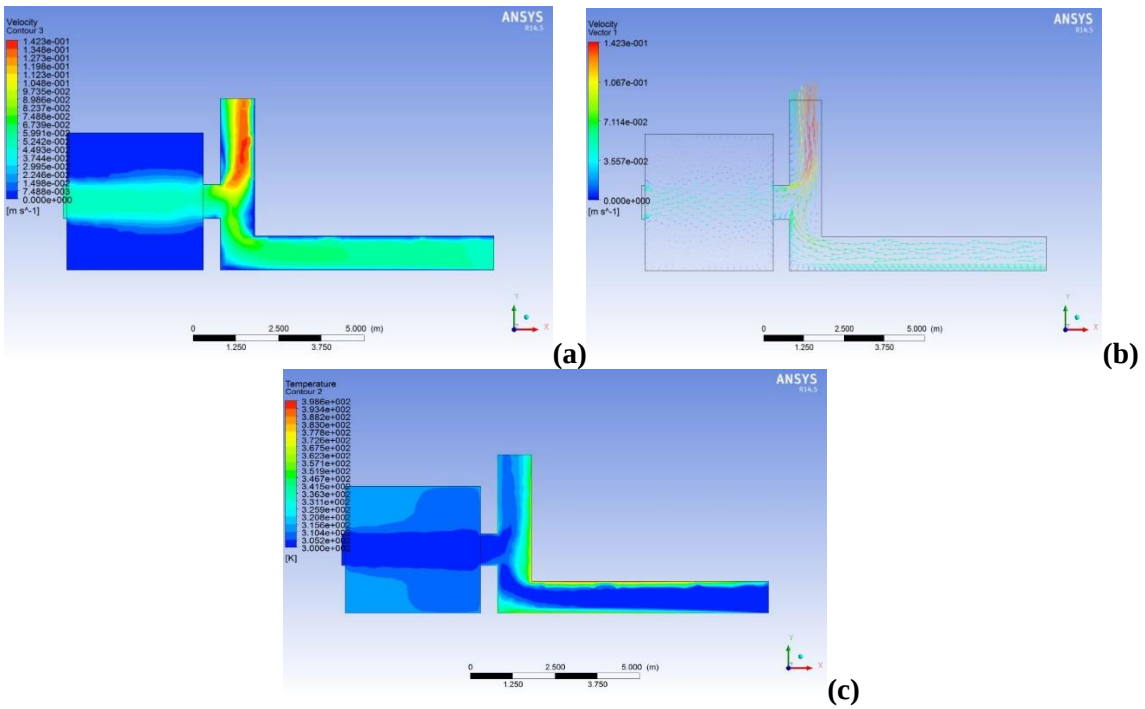

Figure 7. Minimum SC Height Results Visualisation (a) Velocity Contour (b) Velocity Vector (c) Temperature Contour

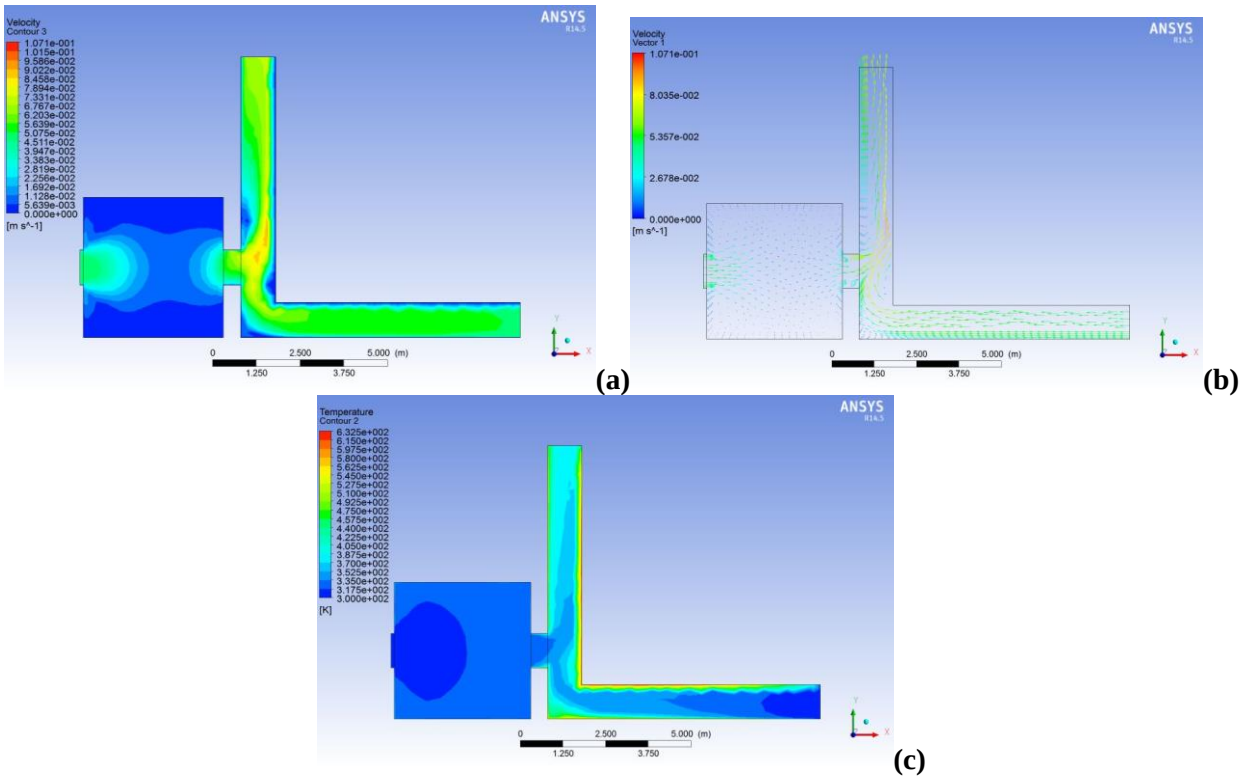

Figure 8. Maximum SC Height Results Visualisation (a) Velocity Contour (b) Velocity Vector (c) Temperature Contour

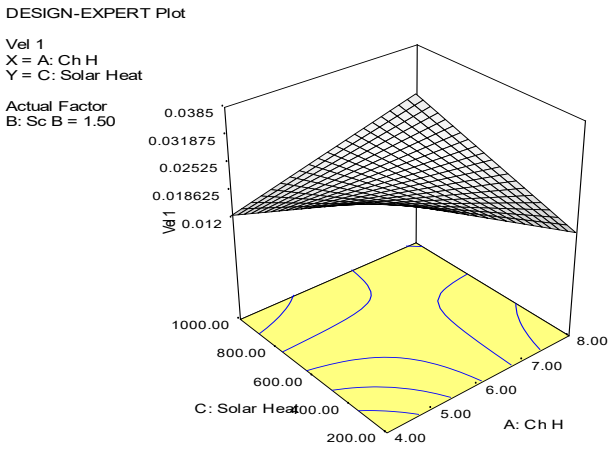

Figure 9. Room Average Velocity (Velocity 1) Interaction 3D Plots of Chimney Height and Solar Heat Flux

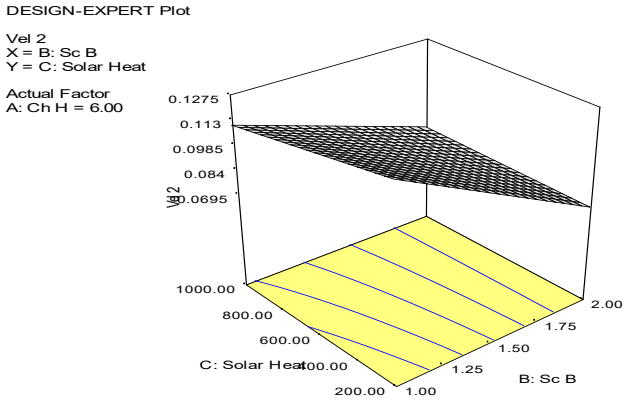

Figure 10. Chimney Average Velocity (Velocity 2) Interaction 3D Plots of Solar Collector Breadth and Solar Heat Flux

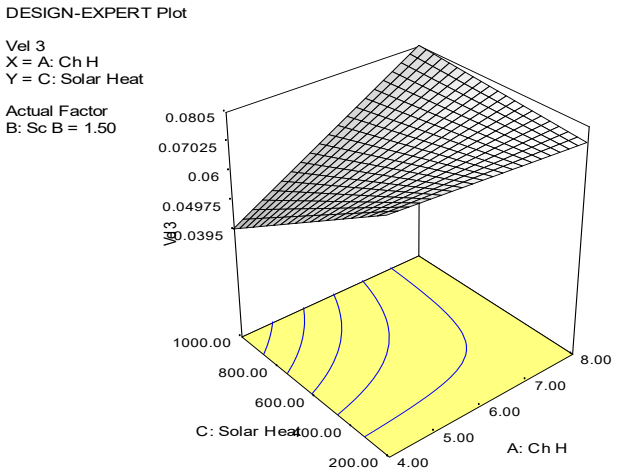

Figure 11. Solar Collector Average Velocity (Velocity 3) Interaction 3D Plots of Solar Heat Flux and Chimney Height

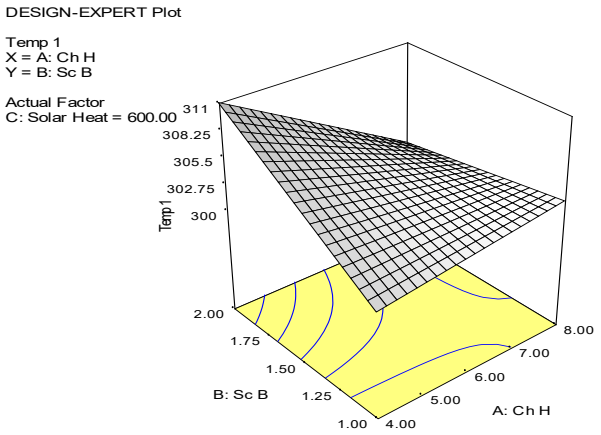

Figure 12. Room Average Temperature (Temperature 1) Interaction 3D Plots of Solar Collector Breadth and Chimney Height

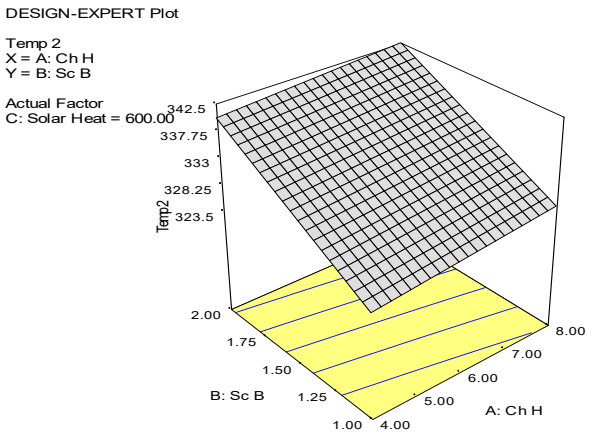

Figure 13. Chimney Average Temperature (Temperature 2) Interaction 3D Plots of Solar Collector Breadth and Chimney Height

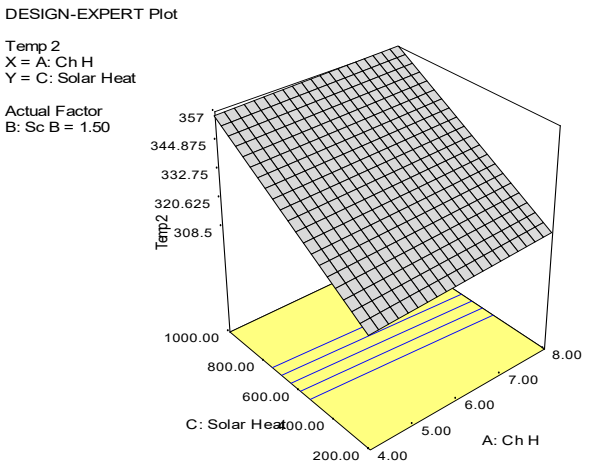

Figure 14. Chimney Average Temperature (Temperature 2) Interaction 3D Plots of Solar Heat Flux and Chimney Height

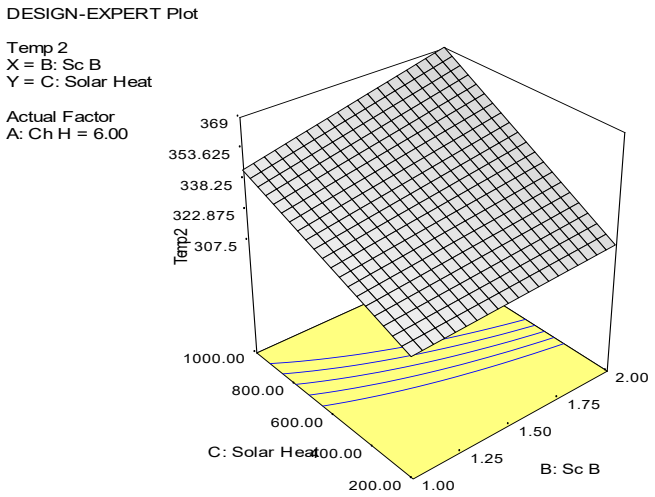

Figure 15. Chimney Average Temperature 2 Interaction 3D Plots of Solar Collector Breadth and Solar Heat Flux

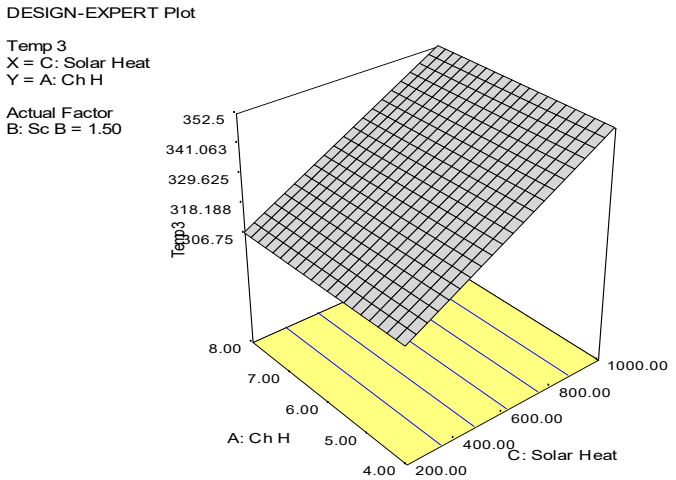

Figure 16. Solar Collector Average Temperature (Temperature 3) Interaction 3D Plots of Solar Heat Flux and Chimney Height

Analysis of Room Average Velocity

From the analysis, it was observed that the interaction factor AC (interaction factor of the chimney height (Factor A) and solar heat flux (Factor C)) has the major influence on the response of the room velocity (Velocity 1). AC contributes 39.81% to the response of Velocity 1. This implies that the chimney height (Factor A) and the solar heat flux (Factor C) determine majorly the conditions in the room as shown in Equation (10). The Interaction Graph Figure 9 shows that the optimised value of the response Velocity 1 occur somewhere between 600 W/m^2 – 800 W/m^2 solar heat flux and 6m – 7m Chimney Height.

Analysis of Chimney Average Velocity

The results show that the size of the solar collector breadth (Factor B) has the major influence on the response of the chimney velocity (Velocity 2). Factor B contributes about 88% to the response

of the chimney velocity (Velocity 2). This implies that the size of the solar collector breadth (Factor B) determines majorly the conditions in the chimney. Though it is expected from theory that the solar heat flux should be of great influence, the result shows that this influence is affected by the breadth of the solar collector. This indicates that the condition in the chimney is optimised as the dimension of the breadth of the solar collector changes as shown in Equations (11). The chimney average velocity is determined by the solar collector breadth (Factor B), this is in agreement with the results of Tan and Wong, (2013). The Interaction Graph Figure 10 shows that the optimised value of the response Velocity 2 (chimney velocity) occurs somewhere between 1.75m – 2.0m solar collector breadth with respect to the solar heat flux.

Analysis of Solar Collector Velocity

The results show that the interaction factor AC of the chimney height (Factor A) and the solar heat flux (Factor C) has the major influence on the response of the average velocity in the (horizontal) solar collector (Velocity 3). AC contributes about 22.9% to the response of the velocity inside the (horizontal) solar collector. This implies that the chimney height (Factor A) and the solar heat flux (Factor C) determine majorly the conditions in the solar collector. It is noted that each factor on its own contributes about 14.8% and 13.2% respectively to the response of Velocity 3. This effect may not have been noticeable if the vary one factor fix other factors experiment was carried out. It is also noted that the results show that the interaction of all the factors also has an effect on this response as expressed in Equations (12). For the case of Velocity 3, Figure 11 shows that increasing chimney height results in corresponding increase in the response of the solar collector velocity (Velocity 3), this is in agreement with the results of the many researchers in the solar chimney power plant (SCPP) systems (Pretorius and Kröger, 2007; Zhou *et al*., 2010a). The Interaction Graph Figure 11 shows that the optimised value of the response Velocity 3 occurs somewhere between 200 W/m^2 – 400 W/m^2 solar heat flux and 7 m – 8 m chimney height.

Analysis of Room Temperature

It was observed that the interaction factor AB of the chimney height (Factor A) and the solar collector breadth (Factor B) has the major influence on the room temperature (Temperature 1). AB contributes about 36.76% to the response of Temperature 1, while Factors A, B, AC and BC contribute 14.57% equally to the response of Temperature 1. This implies that the chimney height (Factor A) and the solar collector breadth (Factor B) determine majorly the temperature conditions in the room. It is noted that factors A, B, AC, and BC also show equal influence on the response, this implies that these factors and interactions should also be considered in design; however interaction factor AB is the determining factor of the room temperature as shown in Equation 13. This effect may not have been noticeable if the vary one factor fix other factors experiment was carried out. For the case of Temperature 1 a temperature drop was observed with increasing chimney height, and an increase in temperature was observed with increasing breadth (depth) in agreement with Burek and Habeb, (2007). The Interaction Graph Figure 12 shows that the optimised value of the room temperature (Temperature 1) occurs somewhere between 7 m – 8 m Chimney Height and 1 m – 1.25 m solar collector Breadth.

Analysis of Chimney Temperature

Results indicate that the solar heat flux (Factor C) has the major influence on the response of the chimney temperature (Temperature 2). The solar collector breadth (Factor B) shows a slight influence of about 10.5% to the response of the chimney temperature (Temperature 2). This

implies that the solar heat flux (Factor C) is the dominant factor while the solar collector breadth (Factor B) only contributes to this factor. Therefore, these factors (C and B) should be given priority to in the design of the chimney for effective performance, as shown in Equation (14). A slight chimney temperature drop was observed with increasing chimney height, an increase in temperature was observed with increasing breadth (depth) in agreement with Burek and Habeb, (2007). However, the temperature response for solar heat flux shows a sharp increase with increasing solar heat flux. The Interaction Graphs Figure 13 – 15 show the interaction factors' influence on the chimney temperature (Temperature 2).

Analysis of Solar Collector Temperature

The solar heat flux (Factor C) has the major influence on the response of the (horizontal) solar collector temperature (Temperature 3). This implies that the solar heat flux (Factor C) is the dominant factor and therefore should be attended to in design as implied from Equations (15). For the case of Temperature 3 the solar collector temperature shows a sharp temperature increase with increasing solar heat flux, in agreement with results from Sangi *et al*., (2011), and many other researchers studying solar chimney power plant (SCPP).

Analysis of Optimised Model

The optimisation criteria for the model constraints are as shown below. The chimney height and the solar collector breadth were set within the range of the experimental value; the solar heat flux was set to be minimised between 200 W/m^2 and 600W/m^2; the velocity at points 1 to 3 were maximised; the Temperature at point 1 (Room Temperature) was minimised, while the Temperatures at points 2 and 3 (chimney and solar collector) were set to be maximised.

Optimisation Criteria for the Model

- Chimney Height (Ch H) — Within Range (4 m – 8 m)
- Solar Collector Breadth (Sc B) — Within Range (0.5 m – 1 m)
- Solar Heat Flux — Minimum (200 Wm^{-1} – 1,000 Wm^{-1})
- Velocity 1 (Room Velocity) — Maximum (0.007 ms^{-1} – 0.07 ms^{-1})
- Velocity 2 (Chimney Velocity) — Maximum (0.069 ms^{-1} – 0.12 ms^{-1})
- Velocity 3 (Solar Collector Velocity) — Maximum (0.009 ms^{-1} – 0.09 ms^{-1})
- Temperature 1 (Room Temperature) — Minimum (300 K – 305 K)
- Temperature 2 (Chimney Temperature) — Maximum (305 K – 370 K)
- Temperature 3 (Solar Collector Temperature) — Maximum (300 K – 358 K)

The optimised response parameters show that the Room Temperature (Temperature 1) is conserved and maintained at the minimum value of 300 K, though the Room Velocity (Velocity

1) seems to have reduced to about 0.031 m/s at the point chosen for analysis from 0.05 m/s induced at the window into the room, however, there are other points within the room that show increase in velocity. Moreover, the ability of the system to maintain the room temperature despite the reduction in velocity at the point chosen for analysis is as a result of other points within the room experiencing increase and the increase in velocity at the room cavity section as the room air enters the chimney, which is due to the increase in velocity in the chimney from 0.05 m/s to about 0.12 m/s in both optimised models. This is as desired. The chimney temperature (Temperature 2) is found to have increased from 300 K to about 314.7 K and 315.1 K in both solutions respectively.
The velocity in the solar collector at point 3, which is the junction between the chimney and the horizontal solar collector, also shows an increase in velocity from 0.05 m/s to about 0.07 m/s in both optimised solutions. However, it was observed that for power generation putting the turbine at a position close to the top of the chimney will be more desirable, since that is where the velocity is at the maximum.
Moreover, from the review of literature and according to Gontikaki *et al.*, (2010), wind is a highly influential climatic parameter; its effect is a major contributor to the effectiveness of a solar chimney system and would improve the results gotten from the optimised model.

Effect of Wind on the Optimised Model

The effects of induced wind of 1 m/s from two positions were simulated; induced wind at the room inlet and at the (horizontal) solar collector inlet. Induced wind from both inlets simultaneously was also simulated as shown in Figure 17.

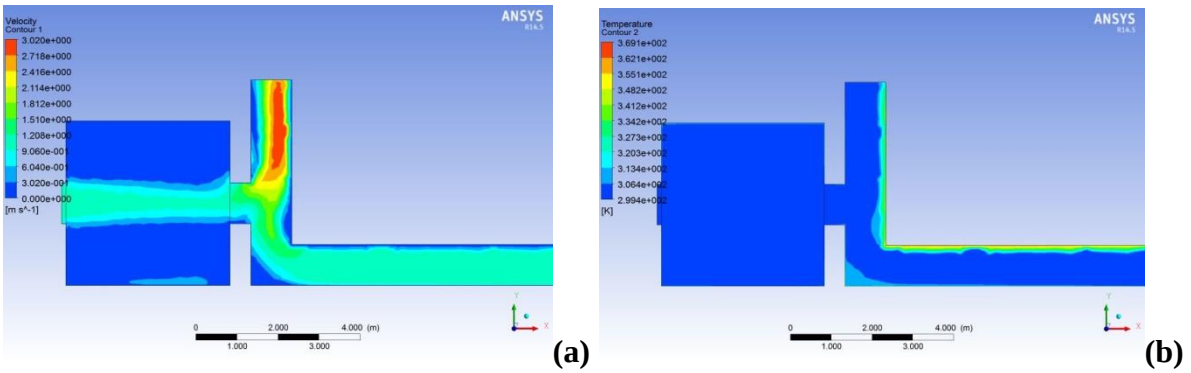

Figure 17. Wind Effect from Both the Room and Solar Collector Inlet (a) Velocity Contour (b) Temperature Contour

Wind Effect from Room Inlet

It was observed that positioning the room openings in the direction of the wind improved the flow within the room. The velocity distribution within the room ranging from about 0.098 m/s to about 1.3 m/s at the centre of the room, producing an Air Change rate of between 5.51 to 73.13 respectively which is comparable with results of other researchers (Tan and Wong, (2014); Mathur *et al.*, (2006)); the temperature within the room is maintained fairly at 300 K. The Rayleigh number for the room is 1.63 x 10^{10}, and Nusselt number is 186.6. The velocity distribution within the chimney ranges from about 0.09 m/s at the bottom to about 1.6 m/s at the top. Positioning the wind turbine at the top will be ideal in this case.

Wind Effect from Horizontal Solar Collector Inlet

It was observed that positioning the horizontal solar collector opening in the direction of the wind improved the flow within the room slightly from 0.05 m/s to about 0.186 m/s. The velocity distribution within the room shows a uniform distribution of about 0.186 m/s producing an Air Change rate of 10.46, which is still comparable with results of other researchers (Tan and Wong, (2014); Mathur *et al*., (2006)); the temperature range within the room is between 299 K at the centre of the room to 334 K at the towards the bottom, this is as a result of the air change at the centre of the room directly facing the window and the room-chimney exit and stale hot air trapped at the bottom of the room. Points at the top of the room have temperatures reaching up to 355 K as expected. The Rayleigh number for the room is 2.18×10^{10}, and Nusselt number is about 200. The velocity distribution within the chimney ranges from about 0.9 m/s to about 1.5 m/s ideal for energy harnessing.

Wind Effect from Both the Room Inlet and the Horizontal Solar Collector Inlet

It was observed that positioning both the room inlet and the horizontal solar collector inlet in the direction of the wind improved the flow within the room from the induced wind of 1.0 m/s to about 1.5 m/s at the centre of the room producing an Air Change rate of between 16 and 84 respectively, comparable with results of other researchers (Tan and Wong, (2014); Mathur *et al*., (2006)); the temperature range within the room is about 299 K. The Rayleigh number for the room is 2.18×10^{10}, and Nusselt number is about 200 which are similar results when the wind is induced from the horizontal solar collector opening alone. The velocity distribution within the chimney ranges from about 1.2 m/s to about 3 m/s which is very ideal for power generation.

Further Analysis

Room Conditions

In the room, the influencing factor(s) on the velocity and temperature was observed to be different. The room velocity is mainly affected by the interaction between the chimney height (A) and the solar heat flux (C), while the room temperature is mainly affected by the interaction of the chimney height (A) and the solar collector breadth (B) though other factors have a bit of influence as evident from the room temperature equation (Equation 19). It is inferred from this situation that the value of Factor B is important and serves as a limiting and determining factor for the flow and temperature conditions in the room. A change in the value of B will cause a change in the value of the interaction factor AC, which may lead to change in the room velocity. Burck and Habeb (2007) noted that the room mass flow rate is a function of depth, while Tan and Wong (2013) stated that the solar chimney depth has similar effect on the mass flow as the width. However, Tan and Wong (2013) reported a decrease in the mass flow as the width is increased, which is similar to the observation of the present study; furthermore, they noted that at a stack height to width ratio of less than 7 produces an increase in mass flow in their two-dimensional flow analysis with an increase in the width; Gontikaki *et al*., (2010) also made similar observation earlier. These observations further iterate the importance of the effect of the interaction factors in the analysis of the solar chimney system.

Solar Chimney Conditions

In the chimney the dominating factors are the solar collector breadth (Factor B), which also determine the breadth of the chimney, for the chimney velocity and solar heat flux (Factor C) for temperature of the chimney. It was however, observed from the equation of the Chimney velocity, Equation 17, that the importance of factor B (width) is a function of interaction of the solar heat

flux (C) and the width. This implies that an increase in the width will produce an increase in the chimney velocity (Velocity 2), which is desirable for the purpose of power generation, however, may lead to a decrease in the room velocity, which is not so desirable.

Horizontal Solar Collector Conditions

In the Solar Collector the domination factors are the interaction factor of the Chimney height (A) and the Solar heat flux (C) collector velocity (Velocity 3) and the solar heat flux (C) for the temperature of the collector. It is however, observed from, Equation 18 and Equation 21, that the Solar heat flux plays a very important role in the determination of the conditions of point 3 in the Solar Collector. This is as expected.

4 CONCLUSION

The aim of the study is the development and optimisation of a Solar Chimney (SC) model for the dual purpose of passive ventilation and renewable power generation in buildings in tropical conditions. To achieve this, a theoretical model of the combined ventilation and power solar chimney was developed, which was simulated using the ANSYS-Fluent commercial CFD software. An optimised model was arrived at by conducting a 2^3 Factorial designed experiment for the sensitivity analysis and determination of the interactions of factors, if any, among the main factors and thus the optimised model. Comparison of the results obtained for the proposed "Ventapower" SC and other validated simulation research works were done. Improvements were observed in the "Ventapower" system thermal performance and sufficient flow speed achieved in the chimney for the purpose of power generation. Results obtained show that factorial experiment revealed the effect of interactions of parametric factors of the SC (chimney height, width and solar heat flux), and these parameters were of great importance in the performance of the SC. The system also shows a great dependence on the ambient wind conditions. The power output from the SC was about 25 W/m^2, with a channel velocity of 1.5 m/s. The room temperature was maintained fairly as its initial value of 300 K, with an increase in room velocity to about 1.5 m/s.

5 ACKNOWLEDGEMENTS

Dr. Zaki El Hasan, University of the West of Scotland (Assistance with ANSYS Fluent)
Dr. Bob Baileys, University of the West of Scotland (Assistance with ANSYS APDL Workbench)
Prof. Abraham Ogwu, University of the West of Scotland (Assistance with the Design of Experiment)
Mr. Israel Ruuwan, Nigeria (Assistance with ANSYS Fluent)

6 REFERENCES

1. ANSYS FLUENT Theory Guide (2011) ANSYS, Inc., Southpointe, 275 Technology Drive, Canonsburg, PA 15317, ansysinfo@ansys.com, http://www.ansys.com ANSYS, Inc. Release 14.0 November 2011
2. Alwetaishi, M. (2017). Impact of glazing to wall ratio in various climatic regions: A case study. *Journal of King Saud University – Engineering Sciences*, http://dx.doi.org/10.1016/j.jksues.2017.03.001

3. Alwetaishi, M., Balabel, A. (2017). Numerical study of micro-climatically responsive school building design in Saudi Arabia. *Journal of King Saud University – Engineering Sciences*, http://dx.doi.org/10.1016/j.jksues.2017.03.005
4. Arce J., Jimenez M.J., Guzman J.D., Heras M.R., Alvarez G., Xaman J., (2009). Experimental study for natural ventilation on a solar chimney. *Renewable Energy* 34 (2009) 2928–2934.
5. Bar-Cohen, A., Krauss, A.D., (1988). Advances in Thermal Modeling of Electronic Components and Systems. Hemisphere Publishing Corporation, New York.
6. Ben Sills (Aug 29, 2011). "Solar May Produce Most of World's Power by 2060, IEA Says". *Bloomber http://www.bloomberg.com/news/2011-08-29/solar-may-produce-most-of-world-s-power-by-2060-iea-says.html* (viewed 1st Nov. 2012)
7. Bilgen E. and Michel J. (1979), 'Integration of solar systems in Architectural and Urban Design' Chapter 19, Solar Energy Applications in Buildings (Editor A. A. M. Sayigh), Plenum Press, New York, pp. 279–296.
8. Burek S.A.M., Habeb A., (2007). Air flow and thermal efficiency characteristics in solar chimneys and Trombe Walls. *Energy and Buildings* 39 (2007) 128–135.
9. Chena Z.D., Bandopadhayay P., Halldorsson J., Byrjalsen C., Heiselberg P., Li Y., (2003). An experimental investigation of a solar chimney model with uniform wall heat flux. *Building and Environment* 38 (2003) 893 – 906
10. Ekechukwa, O.V., Norton, B., (1999). Review of solar energy drying system II. An overview of solar drying technology. *Energy Conversion & Management*. 40, 615–655.
11. Gontikaki M., Trcka M., Hensen, J.L.M. & Hoes P. (2010). Optimization of a solar chimney design to enhance natural ventilation in a multi-storey office building. Proceedings of 10th International Conference for Enhanced Building Operations, Kuwait: ICEBO.
12. Ikhile C. I., (2012). The Impact of Climate Change on the Discharge of Osse-Ossiomo River Basin, South Western Nigeria under Different Climatic Scenarios. *International Journal of Science and Technology*, Bahir Dar, Ethiopia, Volume 1: 208 – 220
13. Jamalabadi, M.Y. Abdollahzadeh, (2014). Experimental investigation of thermal loading of a horizontal thin plate using infrared camera. *Journal of King Saud University – Engineering Sciences*, 26: 159–167
14. Layeni, A. T., Waheed, M. A., Jeje, O. O., Giwa, S. O. (2015). Computational Analysis of a Dual Purpose Solar Chimney for Buildings in Nigeria. Proceedings of the 8th International Conference on Sustainable Energy & Environmental Protection (SEEP2015), Paisley, August 11-14, 2015, 8(1), Pages 363 – 369.
15. Layeni, Abayomi T., Waheed, M. Adekojo, Adewumi, Babatunde A., Bolaji, Bukola O., Nwaokocha, Collins N., Giwa, Solomon. O. (2020a). Computational modelling and simulation of the feasibility of a novel dual purpose solar chimney for power generation and passive ventilation in buildings, Scientific African, 2020. 8 (2020a) e00298. https://doi.org/10.1016/j.sciaf.2020.e00298
16. Layeni Abayomi, Collins Nwaokocha, Olalekan Olamide, Solomon Giwa, Samuel Tongo, Olawale Onabanjo, Taiwo Samuel, Olabode Olanipekun, Oluwasegun Alabi, Kasali Adedeji, Olusegun Samuel, Jagun Zaid Oluwadurotimi, Olaolu Folorunsho, Jacob Adebayo and Folashade Oniyide (2020b). Computational Analysis of a Lecture Room Ventilation System. Chapter in the Book, Zero-Energy Buildings, IntechOpen, London, UK**.** pp. 77 – 101. DOI: http://dx.doi.org/10.5772/intechopen.92725. [Web of Science]

17. Lee Joyce, Zhao Feng (2020). GWEC | GLOBAL WIND REPORT 2019. Global Wind Energy Council. Rue Belliard 51-53 1000 Brussels, Belgium. Published 25 March 2020. https://gwec.net/global-wind-report-2019/
18. Liu Wei, Ming Ting-Zhen, and Yang Kun, (2005). Simulation of Characteristics of Heat Tranfer and Flow for MW Grade Solar Chimney Power Plant. Proceedings of ISEC 2005, International Solar Energy Conference, August 6-12, 2005, Orlando, Florida. ISEC 2005-76221.
19. Mathur Jyotirmay, Bansal N.K., Mathur Sanjay, Jain Meenakshi, Anupma, (2006). Experimental investigations on solar chimney for room ventilation. *Solar Energy*, 80: 927–935.
20. Morales, Alex (2012), Wind Power Market Rose to 41 Gigawatts in 2011, Led by China, Posted February 07, 2012 http://www.businessweek.com/news/2012-02-07/wind-power-market-rose-to-41-gigawatts-in-2011-led-by-china.html (viewed 1st Nov. 2012)
21. Nouanégué H.F., Bilgen E., (2009), Heat transfer by convection, conduction and radiation in solar chimney systems for ventilation of dwellings, *International Journal of Heat and Fluid Flow* 30 150–157 (2009).
22. Nwofe P. A. (2014) Utilization of Solar and Biomas Energy-A Panacea to Energy Sustainability in a Developing Economy. *International Journal of Energy and Environmental Research*. Vol. 2 No. 3 Pp 10 – 19
23. Peri Aditya, Fernandes Priam Mario and Vishwanadha Chandrashekhar, (2011). Numerical Simulation of Air Flow in a General Ward of a Hospital. International Journal of Research and Reviews in Applied Sciences 8 (3) 400 – 444.
24. Pretorius J. P. and Kröger D. G., (2009). The Influence of Environment on Solar Chimney Power Plant Performance. *R & D Journal, of the South African Institution of Mechanical Engineering* 2009, 25. http://www.saimeche.org.za (open access)
25. Pretorius, J. P. (2007). Optimization and Control of a Large-scale Solar Chimney Power Plant. Dissertation presented for the degree of Doctor of Mechanical Engineering at the University of Stellenbosch. March 2007.
26. Pretorius, J. P., and Kröger, D. G. 2007. Sensitivity analysis of the operating and technical specifications of a solar chimney power plant, Journal of Solar Energy Engineering,Transactions of the ASME, 129: 171-178.
27. Pretorius, J. P., and D. G. Kröger (2006), Critical evaluation of solar chimney power plant performance, *Solar Energy*, *80*, 535-544.
28. Renewables 2011 Global Status Report (2011) http://www.ren21.net/Portals/97/documents/GSR/GSR2011_Master18.pdf (viewed 1st Nov. 2012)
29. Sangi Roozbeh, Amidpour Majid, Hosseinizadeh Behzad, (2011). Modeling and numerical simulation of solar chimney power plants. *Solar Energy* 85 (2011) 829–838
30. Schlaich J. (1995). The solar chimney: electricity from the sun. Stuttgart, Germany: A. Menges; pp 16, 1995.
31. Schlaich Jörg and Schiel Wolfgang (2000), Solar Chimneys, Encyclopedia of Physical Science and Technology, Third Edition 2000. Schlaich Bergermann und Partner, Consulting Engineers, Stuttgart.
http://citeseerx.ist.psu.edu/viewdoc/download?doi=10.1.1.454.1346&rep=rep1&type=pdf
(Viewed 1st November 2012, 1st October 2015)

32. Tan Alex Yong Kwang and Wong Nyuk Hien, (2013). Parameterization Studies of Solar Chimneys in the Tropics. *Energies* 2013, *6*, 145-163
33. Tan Alex Yong Kwang, and Wong Nyuk Hien, (2014). Influences of ambient air speed and internal heat load on the performance of solar chimney in the tropics. *Solar Energy* 102 (2014) 116–125
34. United Nations Environment Programme *Global Trends in Sustainable Energy Investment 2007: Analysis of Trends and Issues in the Financing of Renewable Energy and Energy Efficiency in OECD and Developing Countries,* sefi.unep.org/fileadmin/media/sefi/docs/publications/SEFI_Investment_Report_2007.pdf (viewed 1st Nov. 2012)
35. Zhou X. P., Yang J. K and Xiao B., (2007a) Improving natural ventilation in combined solar house with solar chimney and solar water collector, *Journal of the Energy Institute* 80-1 55–59 (2007)
36. Zhou Xinping, Wanga Fang, Ochieng Reccab M., (2010a). A review of solar chimney power technology. *Renewable and Sustainable Energy Reviews*, 14 (2010) 2315–2338
37. Zhou Xinping, Yang Jiakuan, Wang Fen, Xiao Bo, (2009b). Economic analysis of power generation from floating solar chimney power plant. *Renewable and Sustainable Energy Reviews* 13 (2009) 736–749.
38. Zhou Xinping, Yang Jiakuan, Xiao Bo, Hou Guoxiang, Xing Fang, (2009) Analysis of chimney height for solar chimney power plant. *Applied Thermal Engineering* 29 (2009) 178–185.